



their signals with a sampling frequency set to  $f_{MDDS}$ , then down converts, filters and passes them to the DSP. A 310 ns analogue delay is applied to the PhPU signal to equalise the group delays in the PhPU and the CR paths. The phase and radial loop sampling frequencies are 90 kHz and 12.7 kHz, respectively. The phase loop is AC-coupled, with a cut-off at 10 Hz to reduce static frequency errors associated with a DC-coupled phase loop. A laptop runs the DSP and uploads the code to FPGAs and DSP.

## HARDWARE

The DSP carrier board [6] is a 6U VME board with a 32-bit slave interface. It hosts four FPGAs, one ADSP21160 DSP and two memory blocks. The daughter boards are based on Altera FPGAs. The MDDSC runs at up to 35 MHz. The MDDS uses an Analogue Devices' AD9754 digital/analogue converter, a 14-bit resolution device capable of generating outputs with update rates of up to 125 MHz. The SDDS daughter board is similar to the MDDS daughter board, apart from the output antialiasing filter. The four-channel DDC daughter board carries four 14 bit, 80 MHz Analog Devices AD9245 analogue/digital converters, clocked by the MDDSC. L1 to L4 are antialiasing filters. The C02 cavity works in the frequency range 0.6 - 1.8 MHz thus allowing operating at the RF harmonic  $h=1$  [5]. The RPU is based on metallised ceramic tubes with sandblasting-formed electrodes. It is provided with a sum ( $\Sigma$ ) and four difference ( $\Delta$ ) electrodes. The PhPU is described elsewhere [7,8].

## SOFTWARE

### FPGA

The FPGA code deployed for the DSP carrier board implements the board VME interface and address decoding, a  $B_{up}/B_{down}$  counter and a DSPSC counter. It also generates an interrupt on the DSP. The DDC FPGA code implements a programmable DDC, which includes a decimating Cascaded-Integrator-Comb (CIC) filter. By developing the DDC in FPGA the group delay is minimised, an important feature in a feedback loop. The CIC parameters are set to different values depending on the channel and on its use. The same FPGA code for the MDDS and SDDS implements a digital synthesiser.

### DSP

The DSP code performs three tasks, executed as interrupt service routines. The slow-loop task carries out background jobs, such as cycle-start DSP initialisation and DSP data refresh. The internal DSP timer triggers it every  $T_{SL} = 1$  ms. The fast-loop task is responsible for core activities such as phase and radial loops, radial steering, frequency program execution and  $f_{MDDS}$  updating. The DSPSC triggers it every  $T_{FL} = 11.1$   $\mu$ s. The external timing task initialises several parameters and starts the DSP beam control for the next cycle. It is triggered by the start cycle RTM timing input.

The DSP implements a novel approach [3] to the

generation of vector based reference-functions and timings, indicated here as soft-GFAS and soft-timings, respectively. These are functions traditionally generated by VME hardware as analogue output. We also developed DSP-Oasis, a user-selectable digital data acquisition function providing diagnostic and troubleshoot access points to check real-time data and to save them for later analysis.

The system prototype implements frequency program, radial steering, phase and radial loops capabilities. In the frequency program, the injection frequency is user-selected to optimise the capture process. After a soft-timing, the frequency program shifts to using the  $B_{up}$  and  $B_{down}$  values. The radial steering is implemented via a soft-GFAS. The phase loop, closed by a soft-timing, is AC-coupled via a low-pass, first order IIR filter. The radial loop, closed by a soft-timing, uses a Proportional-Integral regulator (PI) allowing two different settings in one cycle.

## BEAM CONTROL TESTS

The beam controlled with the system prototype was injected and accelerated in PSB ring four with the PSB ejection kicker disabled; the beam was not extracted. The beam was kept at low intensity, typically about  $10^{11}$  protons, to avoid triggering the beam loss monitor alarm. On a few occasions, a higher intensity ( $\sim 10^{12}$  protons) was allowed. The phase loop was closed at  $ctime = 275.3$  ms and the radial loop at  $ctime = 282$  ms. In the phase loop tests the radial loop was not closed.

### Capture and Acceleration Efficiencies

The capture and acceleration efficiencies were measured by continuously controlling one user beam and taking snapshots of the operational display. The beam intensity was varied from one cycle to another and the captured particles number range was  $1.4 \cdot 10^{11}$  to  $1.8 \cdot 10^{12}$ . Measured efficiencies were between 95% and 100%, similar to analogue PSB beam control efficiencies.

### Phase Loop Dynamics

In the Phase Loop Dynamics tests, we added a 0.2 rad step-function stimulus to the measured phase error  $\phi_m$ , starting at  $ctime = 285$  ms. This modified  $\phi_m$  was fed to the phase loop and the response was observed by the DSP-Oasis measurement. The radial loop was kept open.

The nominal phase loop bandwidth was 7 kHz. The high and low frequency poles  $f_H$  and  $f_L$  of the closed loop system with the phase loop active were calculated to be 7 kHz and 570 Hz, corresponding to time constants  $\tau_{HPL} = 23$   $\mu$ s and  $\tau_{LPL} = 280$   $\mu$ s. Figure 2 shows the measured phase error  $\phi_m$  versus  $ctime$  and the lower plot highlights the fast time constant of the decaying part of the curve. It was obtained by setting the DSP-Oasis sampling period  $t_{DAQ}$  to  $T_{FL}$ . The measured fast time constant was  $\sim 25$   $\mu$ s. The upper curve has a slow time constant of  $\sim 300$   $\mu$ s, obtained with  $t_{DAQ} = 5 \cdot T_{FL}$ . Both time constants agree with the expected values of  $\tau_{LPL}$  and  $\tau_{HPL}$ .

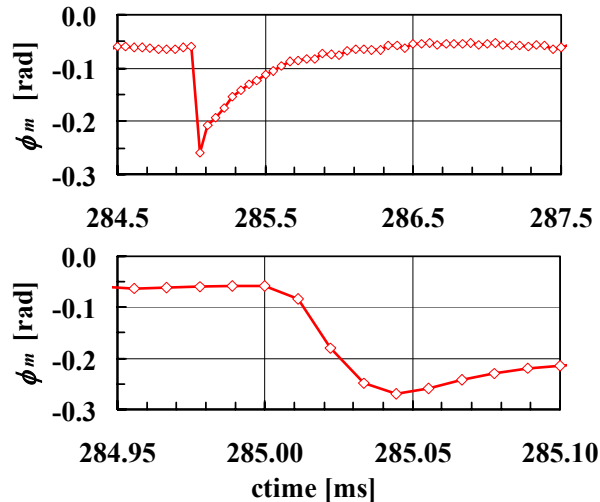


Figure 2: Plots of the phase error  $\phi_m$  versus ctime.

### Radial Loop Dynamics

For the Radial Loop Dynamics tests the two PI settings were optimised for  $ctime = 467$  ms and for  $ctime = 612$  ms. This was achieved by setting the PI regulator zero so as to cancel the phase loop low frequency pole  $f_L$ , at those ctimes. The PI radial loop gains were chosen such that the dominant radial closed loop time constant  $\tau_r$  is 2 ms.

The beam radial position was varied by means of a radial steering reference function with two 5 mm steps: one at  $ctime = 467$  ms and another at  $ctime = 617$  ms. Figure 3 shows the radial position  $r$ , acquired by DSP-Oasis as a function of ctime. The lower plot zooms the upper one on the ctime corresponding to the steep radial position first change. For both plots we set  $t_{DAQ} = 48 \cdot T_{FL}$ . As expected, the radial response time constant was 2 ms.

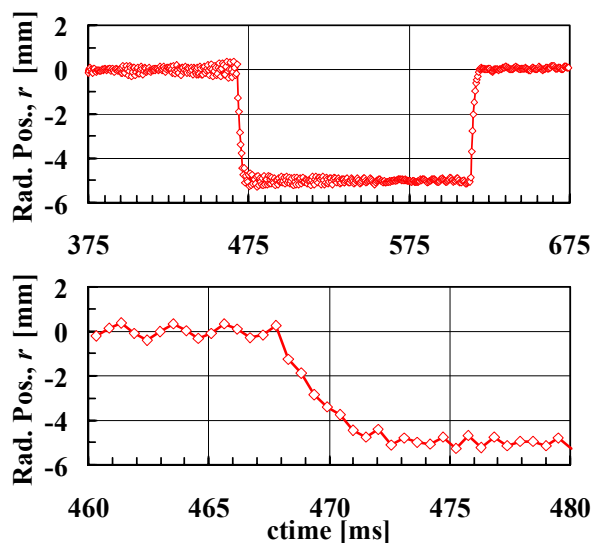


Figure 3: Plots of the DSP-measured radial position as a function of ctime, when a radial steering is applied.

## CONCLUSION AND OUTLOOK

A new beam control system for LEIR is being developed. A set of beam tests has been carried out in the PSB and this paper detailed the system setup deployed, both hardware and software, as well as some test results. The tests were successful in their beam control part and validated several new concepts, such as soft-GFAS, DSP-Oasis and soft-timings. The system proved to be very flexible and performant.

### From Prototype to LEIR

A new version of the MDDS daughter board will implement a tagged clock scheme, to phase-synchronise all daughter boards' numerically controlled oscillators to a common revolution phase reference. A fanout unit will deliver the tagged master clock over cable or optical fibre.

The beam control system will operate the gap relays of the LEIR cavities [9], to short-circuit them when not in use, thus avoiding beam self-bunching due to cavity impedance.

Capabilities such as a cavity voltage envelope control and a beam ejection synchronisation loop will be added. Three DSP carrier boards, communicating with each other by DSP linkports, will interface with all the hardware. A dedicated real time task will run on the PPC, for remote control and data exchange with the user. Suitable application programs will be developed.

### Roadmap After LEIR

After commissioning LEIR, a plan will be finalised to migrate the PSB, Proton Synchrotron and Antiproton Decelerator beam control systems to the LEIR digital scheme, to improve uniformity and maintainability.

## REFERENCES

- [1] M. Chanel, "LEIR: The Low Energy Ion Ring at CERN", EPAC'02, Paris, June 2002, p. 563.
- [2] S. Maury et al, "Ions for LHC: Beam Physics ... Challenges", Paper RPPE005, this conference.
- [3] M. E. Angoletta et al., "PS Booster Beam Tests of the New Digital Control System for LEIR", CERN/AB-Note-2005-017-RF.
- [4] M. E. Angoletta et al., "Feasibility Tests of a New All-Digital Beam Control Scheme for LEIR", CERN/AB-Note-2004-004-RF.
- [5] A. Krusche, M. Paoluzzi, "The New Low Frequency Accelerating Systems For The CERN PS Booster", EPAC'98, Stockholm, June 1998, p. 1782.
- [6] J. DeLong et al., "Topology for a DSP-Based Beam Control System in the AGS Booster", PAC'03, Portland, May 2003, p. 3338.
- [7] G. C. Schneider, "The Phase Pick-Ups and their Signal Transmission in the PSB Beam Control Systems", CERN PS/RF/Note 96-15.
- [8] A. Findlay, "PSB Phase Pickup ... Modifications for 2001", CERN PS/RF/Note 2001-007.
- [9] M. Paoluzzi, "The LEIR RF System", Paper WPAT018, this conference.